Identification of *Cis*-Element Regulating Expression of the Mouse *Fgf10* Gene during Inner Ear Development

Hideyo Ohuchi,[1]* Akihiro Yasue,[1–3] Katsuhiko Ono,[4] Shunsuke Sasaoka,[5] Sayuri Tomonari,[1] Akira Takagi,[1] Mitsuo Itakura,[2] Keiji Moriyama,[3] Sumihare Noji,[1] and Tsutomu Nohno[5]

Fibroblast growth factor (FGF) signaling is crucial for the induction and growth of the ear, a sensory organ that involves intimate tissue interactions. Here, we report the abnormality of *Fgf10* null ear and the identification of a *cis*-regulatory element directing otic expression of *Fgf10*. In *Fgf10* null inner ears, we found that the initial development of semicircular, vestibular, and cochlear divisions is roughly normal, after which there are abnormalities of semicircular canal/cristae and vestibular development. The mutant semicircular disks remain without canal formation by the perinatal stage. To elucidate regulation of the *Fgf10* expression during inner ear development, we isolated a 6.6-kb fragment of its 5′-upstream region and examined its transcriptional activity with transgenic mice, using a *lacZ*-reporter system. From comparison of the mouse sequences of the 6.6-kb fragment with corresponding sequences of the human and chicken *Fgf10*, we identified a 0.4-kb enhancer sequence that drives *Fgf10* expression in the developing inner ear. The enhancer sequences have motifs for many homeodomain-containing proteins (e.g., Prx, Hox, Nkx), in addition to POU-domain factors (e.g., Brn3), zinc-finger transcription factors (e.g., GATA-binding factors), TCF/LEF-1, and a SMAD-interacting protein. Thus, FGF10 signaling is dispensable for specification of otic compartment identity but is required for hollowing the semicircular disk. Furthermore, the analysis of a putative inner ear enhancer of *Fgf10* has disclosed a complicated regulation of *Fgf10* during inner ear development by numerous transcription factors and signaling pathways. *Developmental Dynamics 233: 177–187, 2005.* © 2005 Wiley-Liss, Inc.

Key words: *Fgf10*; enhancer analysis; *cis*-element; mouse genome; chicken genome; transgenic mouse; inner ear development, semicircular canals; *Fgf10* knockout mouse

Received 25 May 2004; Revised 18 October 2004; Accepted 31 October 2004

INTRODUCTION

The vertebrate inner ear forms a highly complex sensory structure responsible for the detection of sound and balance. During embryonic development, the inner ear arises from a simple epithelium adjacent to the hindbrain, the otic placode, which is specified through inductive interactions with surrounding tissues. Embryological evidence shows that the induction of the otic placode is a multistep process, which requires sequential interaction of different tissues, the adjacent neuroectoderm, and underlying mesoderm with the future otic ectoderm. Recent progress has been made to identify some of the molecular

[1]Department of Biological Science and Technology, Faculty of Engineering, University of Tokushima, Tokushima, Japan
[2]Division of Genetic Information, Institute for Genome Research, University of Tokushima, Tokushima, Japan
[3]Department of Orthodontics, University of Tokushima Graduate School of Dentistry, Tokushima, Japan
[4]Division of Neurobiology and Bioinformatics, National Institute for Physiological Sciences, National Institute of Natural Sciences, Okazaki, Japan
[5]Department of Molecular Biology, Kawasaki Medical School, Kurashiki, Japan
Grant sponsor: Ministry of Education, Culture, Sports, Science, and Technology of Japan; Tanabe Medical Frontier Conference.
***Correspondence to: Hideyo Ohuchi, Department of Biological Science and Technology, Faculty of Engineering, University of Tokushima, 2-1 Minami-Jyosanjima-cho, Tokushima City 770-8506, Japan. E-mail: hohuchi@bio.tokushima-u.ac.jp**

DOI 10.1002/dvdy.20319
Published online 11 March 2005 in Wiley InterScience (www.interscience.wiley.com).

players involved in the developmental processes of the inner ear.

Owing to their gene expression patterns and various experimental manipulations, members of the fibroblast growth factor (FGF) gene family, including FGF2, FGF3, FGF8, FGF9, FGF10, and FGF15/19 have been implicated in different stages of inner ear formation in different species (Pirvola et al., 2004; Wright et al., 2004; for reviews, Baker and Bronner-Fraser, 2001; Rinkwitz et al., 2001; Noramly and Grainger, 2002). These FGFs are involved in induction of the otic vesicle or in later development of the inner ear. The involvement of FGF3 in the formation of the otic vesicle has been demonstrated in chicks (Represa et al., 1991; Vendrell et al., 2000). However, knockout of FGF3 in mice still permitted formation of the inner ear (Mansour et al., 1993). Because both FGF3 and FGF10 are present in the early developing otic vesicle with FGF receptor type 2b (FGFR2b; Pirvola et al., 2000), an effective receptor for both ligands (Ornitz et al., 1996), it was speculated that these two FGFs may have redundant roles by means of FGFR2b during induction of the otic vesicle. We and others reported that *Fgf10* null ears were still normal until otic vesicle formation and exhibited a mild abnormality in inner ear development (Ohuchi et al., 2000; Pirvola et al., 2000; Pauley et al., 2003). Recently, double-mutant mice with FGF3 and FGF10 were generated, in which the formation of the otic vesicle was severely reduced. It is thought, thus, that these FGFs act in combination with each other as neural signals for otic vesicle formation (Wright and Mansour, 2003; Alvarez et al., 2003).

Here, we addressed the role of FGF10 in later development of the inner ear by studying the inner ear phenotype in *Fgf10* null mice. Although FGF10 and other FGFs have multiple and redundant roles in inner ear development, it is crucial to identify the individual role of each *Fgf* gene during organogenesis. On the other hand, the morphology of the inner ear is so complicated that deciphering the molecular mechanisms for transcriptional regulation of *Fgf10* will help to elucidate important aspects of the mechanisms involved in inductive events during inner ear formation. So far, there are several reports on regulatory sequences to target the expression of a gene in the developing inner ear. For example, a promoter sequence specific to the inner ear sensory cells (hair cells) has been reported in the gene of unconventional myosin VIIA (Boeda et al., 2001), and enhancers for *Sox2* expression in the nasal/otic placodes were determined (Uchikawa et al., 2003). A regulatory element of the *Fgf3* promoter region was also identified, but whether this element could drive the expression in the otic vesicle was not decisively determined in vivo (Murakami et al., 2001). Taken together with these accumulating studies, the identification of ear enhancer sequences would open up the possibility for the analysis of developing ear transcriptome. We previously reported a transcriptional regulation of the *Fgf10* gene during limb formation by identifying the 2.1-kb 5′-upstream region of *Fgf10* that drives the expression in the limb bud and cartilages (Sasaki et al., 2002). In this study, we further elucidated an upstream *cis*-element regulating–specific expression of *Fgf10* in the inner ear primordia by analyzing its enhancer activity in transgenic mice.

RESULTS AND DISCUSSION

Ears in *Fgf10* Null Mutants

FGF10 mutant mice have been reported to display relatively mild defects in inner ear development (Ohuchi et al., 2000; Pauley et al., 2003). At embryonic day (E) 10.5, inner ears of mutants appear morphologically normal; the endolymphatic duct that is absent from *Fgfr2b* null mice (De Moerlooze et al., 2000) was formed in *Fgf10*null otic vesicle. However, the mutant otic capsule was smaller, indicating some structural defects in the inner ear formation (Ohuchi et al., 2000). This preliminary result led us to examine the ear phenotype at later stages, just before birth, as *Fgf10* null mice die at birth due to the absence of lungs. To better understand the complex morphology of the inner ear, we reconstructed three-dimensional images of the inner ear from histological sections using a computational program (Fig. 1A–C). We found that the major domains of the inner ear, an endolymphatic duct, semicircular canals, a central vestibule, and a coiled cochlea appeared to form in the mutant. However, semicircular canal formation was markedly disrupted in the *Fgf10* null ear; semicircular disks remained without canal formation. The disk showed roughly L-shaped profile with single vertical disk facing medially with a lateral protrusion of the horizontal plate (Fig. 1B). Serial sectioning of the mutant ear showed two separate neuroepithelial layers: one of them was positioned closed to the vestibule or fused with the macula utriculi and the other in the lateral protrusion of the disks (Fig. 1F,F′). Therefore, they may correspond to anterior and lateral (horizontal) crista, respectively. However, we could not find the presence of the posterior crista in the mutant, whereas three distinct sensory epithelia with cupula were observed in the wild-type (Fig. 1D–E′). On the other hand, the sensory area of the vestibule developed morphologically normally in the mutant (Fig. 1G). The length of the cochlea duct and morphogenesis of endolymphatic duct also appeared normal in *Fgf10* null mutants (Fig. 1B,C).

We next investigated the developmental stage that is affected by *Fgf10* inactivation and that leads to the absence of semicircular canal formation. First, the observation was made at E13.5, when the semicircular ducts are well formed in the normal inner ear (Morsli et al., 1998; Fig. 2A,B). The semicircular ducts emerge as bilayered outpocketings of the dorsal vestibular epithelium. Subsequently, the two opposing walls of these outpocketings approach each other to form a so-called fusion plate, in which the epithelial cells first intercalate to form a single layer and then disappear, creating a hollow duct, which will grow and obtain its adult form (Martin and Swanson, 1993). In the *Fgf10* mutants, the walls of the outpocketing generating the anterior semicircular duct remained relatively dilated even at E13.5 (Fig. 2D). Careful observation of serial sections revealed that the formation of anterior and horizontal fusion plates was initiated (Fig. 2E). However, we could not find the formation of the posterior fusion plate. In contrast, the development

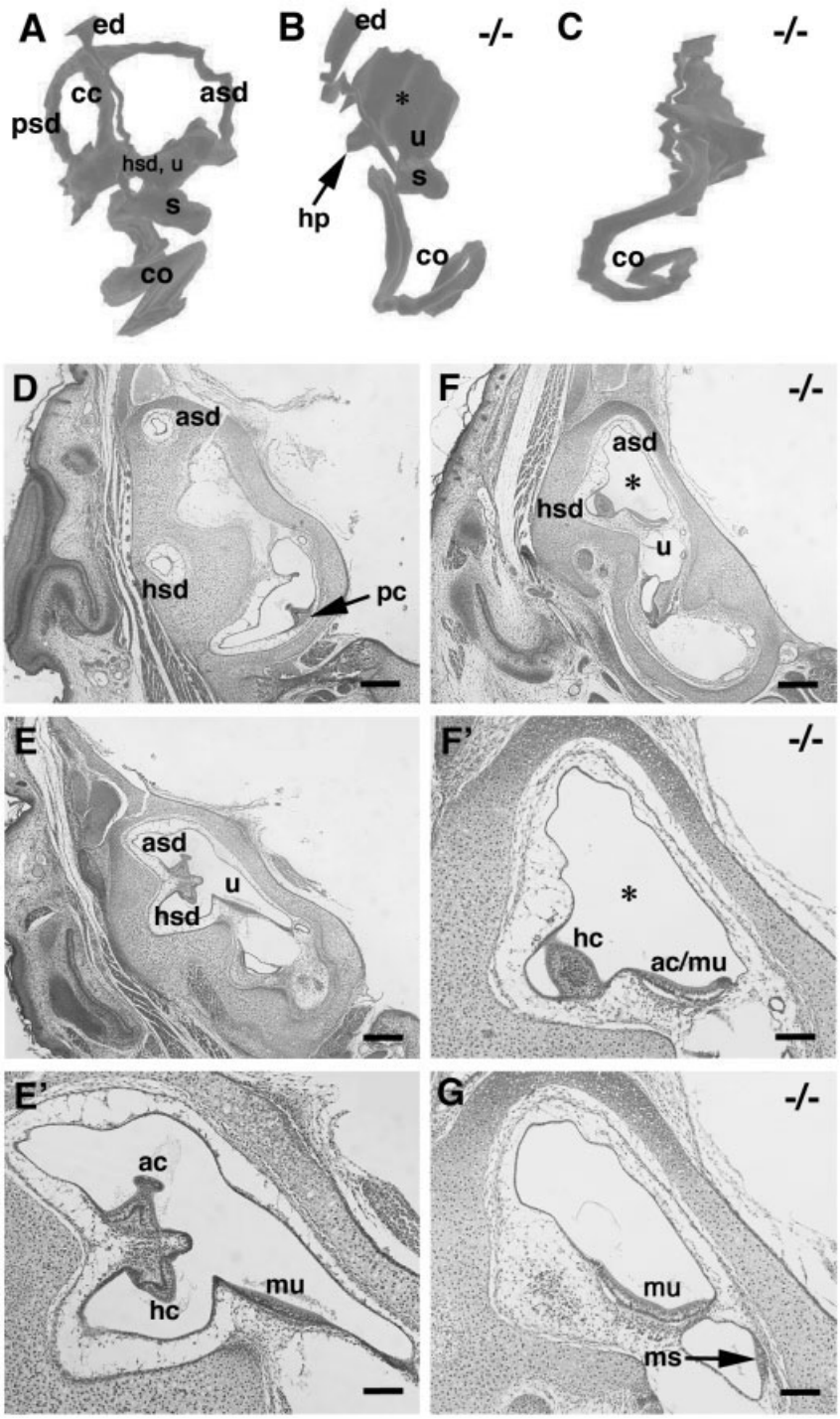

Fig. 1. Disturbed inner ear development in *Fgf10* null mutant mice at late embryogenesis. A–C: Three-dimensional reconstruction of a membranous labyrinth of embryonic day (E) 19 wild-type (A) and age-matched *Fgf10* knockout mice (B,C); medial (A,C) and anteromedial (B) views. The right side is forward the rostral. **A:** The horizontal semicircular duct (hsd) and utricle (u) cannot be distinguished from this angle. **B:** Semicircular disks remain without canal formation (asterisk). **C:** The mutant cochlear duct coils in 1.5 or less than 2 turns as observed in the normal. **D–G:** Transverse sections of E19 otic capsules stained with hematoxylin and eosin. E′,F′ are larger magnifications of E,F, respectively. D,F,F′,G: Typical morphology of semicircular ducts (as shown in D) is missing, and the ducts are replaced by a dilated cavity (asterisks) in the mutant (F,F′,G). D,E,E′,F′: Whereas three distinct sensory epithelia with cupula develop in the wild-type crista ampullaris (D,E,E′), only two of them are observed in the mutant, deformed horizontal crista (hc) and abnormal anterior crista (ac) fused with the macula utriculi (mu). G: The sensory areas of the utricle and saccule develop normally in the mutant. asd, anterior semicircular duct; cc, crus commune; co, cochlea; ed, endolymphatic duct; hp, horizontal plate; ms, macula sacculi; pc, posterior crista; psd, posterior semicircular duct; s, saccule. Scale bars = 100 μm in D–F, 200 μm in E′,F′,G.

of the saccule, cochlear duct, and cochleovestibular ganglion appeared normal in the mutant at E13.5 (Fig. 2C,F).

To further dissect the phenotype of *Fgf10* null inner ear, we compared the expression of two genes, *netrin 1* and *Nkx5.1* (also termed as *Hmx3*) in *Fgf10* mutants and controls. Netrin 1 is a laminin-related protein, whose inactivation leads to the absence of semicircular ducts due to the blockage of fusion plate formation (Salminen et al., 2000). In normal embryos, the opposing walls of the outpocketing giving rise to the anterior semicircular duct are approaching one another at E12.0, and the corresponding fusion plate is formed by E12.5. As reported, *netrin 1* expression was detected in the otic epithelium forming the fusion plates in the normal littermate (Fig. 2G,H). In the mutant, *netrin 1* was expressed, but the extent of the area expressing *netrin 1* seemed decreased and the level of *netrin 1* expression appeared lower in the epithelium (Fig. 2I,J). On the other hand, *Nkx5.1* is a homeobox gene, which is expressed in the developing vestibular structures (Wang et al., 1998). Mice carrying the Nkx5.1 null mutation exhibit severe malformations of the semicircular canals (Hadrys et al., 1998; Wang et al., 1998). In situ hybridization analysis showed that *Nkx5.1* was expressed in the developing vestibular ducts of both controls and mutants at E13.5 (Fig. 2K,L). However, *Nkx5.1* expression appeared down-regulated in the dilated ducts of the mutant (Fig. 2L).

These results suggest that FGF10 is required for semicircular canal morphogenesis, especially in later stages after fusion plate formation, and indispensable for the subsequent removal of the fused cells to proceed with the hollowing of the center of each semicircular plate. Expression of *netrin1* and *Nkx5.1* in the inner ears of *Fgf10* mutants indicates that FGF10 is not required for the initiation of gene transcription of *netrin1* or *Nkx5.1*.

Role of FGF10 in Inner Ear Development

The detailed expression patterns of *Fgf10* and its major receptor *Fgfr2b* have already been reported: *Fgf10* and *Fgfr2b* mRNAs exhibit distinct,

complementary expression patterns in the undifferentiated otic epithelium (*Fgf10* in the ventral epithelium and *Fgfr2b* in the dorsal epithelium; Pirvola et al., 2000). Subsequently, *Fgf10* mRNA becomes confined to the presumptive cochlear and vestibular sensory epithelia and to the neuronal precursors and neuron, while *Fgfr2b* mRNA is expressed in the nonsensory epithelium of the otocyst that gives rise to structures such as the endolymphatic and semicircular ducts (Pirvola et al., 2000). From these expression patterns, it has been concluded that inner ear development depends on paracrine signals that operate within the epithelium. Because *Fgfr2b* is expressed by the presumptive semicircular epithelium and the *Fgf10* null ear exhibits malformation of semicircular canals, FGF10–FGFR2b signaling is likely to mediate some inductive processes from sensory epithelium to nonsensory epithelium during semicircular canal formation. This type of tissue interaction is reminiscent of that observed between the Rathke's pouch and the infundibulum during pituitary development: *Fgf10* is expressed in the infundibulum, whereas *Fgfr2b* is expressed in the Rathke's pouch (Takuma et al., 1998). The anterior pituitary derived from Rathke's pouch is absent from *Fgf10*- or *Fgfr2b*-deficient mice (Ohuchi et al., 2000; De Moerlooze et al., 2000). Furthermore, in otic placode induction, FGF10 has a redundant role with FGF3, as revealed by severely reduced otic vesicles in double mutant mice with *Fgf3* and *Fgf10* (Wright and Mansour, 2003; Alvarez et al., 2003). At this phase of inner ear development, mouse *Fgf10* is expressed in the mesenchyme underlying the prospective otic placode (Wright and Mansour, 2003), indicating that FGF10 signaling mediates epithelial–mesenchymal interactions in early otic development. Thus, it seems likely that FGF10-FGFR2b signaling is involved in dual aspects of tissue interactions during inner ear development.

Inner ear defects of another *Fgf10* null mouse (Min et al., 1998) were examined by Pauley et al. (2003). Our characterization of the *Fgf10* null mutation further has revealed several points. In the absence of FGF10, (1) semicircular plates remain without the hollowing of the center of each semicircular plate; (2) morphogenesis of the cochlear duct (turning, length) occurs normally; (3) expression of *netrin 1* and *Nkx5.1* can be observed in the developing semicircular primordium, showing fusion plate formation initially takes place. Compared with the previously published data, there are the similarities in the inner ear phenotype of these *Fgf10* null mutants as follows; (1) *Fgf10* null mutants show complete agenesis of the posterior crista and the posterior semicircular canal; (2) *Fgf10* mutants have deformations of the anterior and horizontal cristae and reduced formation of the anterior and horizontal canals. Taken together, FGF10 is required for proceeding the removal of the fused cells after semicircular plate formation, especially for the posterior canal formation. The fusion plate cells are thought to be recruited back into the duct epithelium in the mouse (Martin and Swanson, 1993), whereas programmed cell death has been shown to play an important role in removing them in the chick embryo

Fig. 2. Defects at the early stages of inner ear development in *Fgf10* null mutants. A–F: Hematoxylin and eosin–stained transverse sections of embryonic day (E) 13.5 inner ears; the mutants (D–F) show that prominent hypoplasia of the vestibular mesenchyme (m), which is associated with the absence of semicircular ducts, compared with normal littermates (A–C). **A,B:** In normal embryos, the opposing walls of the outpocketing giving rise to the anterior semicircular duct (asd) are approaching one another at E12.0, the corresponding fusion plate is formed by E12.5, and semicircular ducts are well formed by E13.5. **D:** In the mutants, the walls of the outpocketing generating the anterior semicircular duct remain relatively dilated even at E13.5. **E:** Serial sections show that the formation of anterior and horizontal (inset) fusion plates is initiated. **C,F:** The development of the saccule (s), cochlear duct (co), and cochleovestibular ganglion (VIII) appears normal in the mutant at E13.5. G–J: RNA in situ analysis of *netrin 1* expression in normal (wild-type/heterozygote) (G,H) and *Fgf10* null (I,J) ears at E12.5. Transverse sections through anterior (H,J) and posterior (G,I) outpocketings, counterstained with nuclear red. **G,H:** *Netrin 1* expression (in blue) is detected in the otic epithelium forming the fusion plates. **I,J:** In the mutant, the extent of the area expressing *netrin 1* is decreased and the level of *netrin 1* expression appears lower in the epithelium. **K,L:** RNA in situ analysis of *Nkx5.1/Hmx3* expression in normal (wild-type/heterozygote, K) and *Fgf10* null (L) ears. *Nkx5.1* is expressed in the developing vestibular ducts of both controls and mutants at E13.5. *Nkx5.1* expression appears down-regulated in most of the dilated ducts of the mutant, whereas a section of a mutant horizontal semicircular duct (inset in L) exhibits a distinct expression of *Nkx5.1*. ed, endolymphatic duct; fp, fusion plate; hsd, horizontal semicircular duct; psd, posterior semicircular duct; u, utricle. Scale bars = 100 μm in A–L, 50 μm in inset in L.

Fig. 4. Expression of the *lacZ* reporter gene in transgenic embryos with the construct F/*lacZ* (A,B,E–H,J,O), 3-1/*lacZ* (C,I,K,L–N,P), and K/*lacZ* (D). Embryonic days of the mouse embryos are indicated in the right bottom corner of each panel. The arrows in (A,C,D,E,I) show the otic vesicle or ear primordium. **A,C:** By E9.5, construct F drives *lacZ* expression in the otic vesicle (A), while construct 3-1 cannot drive a distinct expression of *lacZ* at this stage (C), as revealed by whole-mount X-gal staining. **B:** Transverse section of the stained transgenic embryo at E10 (construct F, line 53), showing *lacZ* expression in the otic vesicle (ov). Because of greater sensitivity of β-galactosidase detection, the expression seems to expand to a bit more dorsal domain of the otic vesicle than reported on localization of *Fgf10* mRNA (Pirvola et al., 2000). The inset shows a serial section of the same embryo with *lacZ* expression in the emerging ganglion cells (arrowhead). **D:** Construct K cannot drive *lacZ* expression in the otic vesicle. **E:** The E11 embryo (construct F, line 20, also in J) shows *lacZ* expression in the otic vesicle, eyelid, and limb region. F–H: Transverse sections of the stained embryo in E. **F,G:** The *lacZ* expression is found in the sensory epithelia of the semicircular duct and vestibular region (arrows in F,G) and ganglion cells (g in F). **H:** The line 20 embryo also exhibits the expression in the wall of the endolymphatic duct (ed), utriculo-saccular space (us), and cochlear duct (cd). **I:** Construct 3-1 (line 1) drives the expression in the restricted area of the inner ear by E11, compared with construct F. **J:** High-power view of the otic vesicle in E. The *lacZ* expression is found in the endolymphatic duct (arrowhead) and developing crista ampullaris. **K:** High-power view of the otic vesicle in I. Construct 3-1 drives the expression in one side of the endolymphatic duct (arrowhead) and developing horizontal crista. **L:** At E12, more restricted expression in the inner ear is driven by construct 3-1. **M:** Transverse sections of the stained embryo in L. *LacZ* expression in the developing crista (arrow), and ganglion VIII neurons. **N:** *LacZ* expression in the developing macula (arrow), ganglion neurons, and emerging organ of Corti of the cochlea (co). **O:** The *lacZ* expression driven by construct F (line 20) in the endolymphatic duct (arrowhead) and in all three crista. **P:** Construct 3-1 drives *lacZ* expression in more restricted portion of the developing inner ear. ac, anterior crista; asd, anterior semicircular duct; hb, hindbrain; hc, horizontal crista; hv, primary head vein; p, pharynx; pc, posterior crista. Scale bars = 100 μm in B,F–H,M,N.

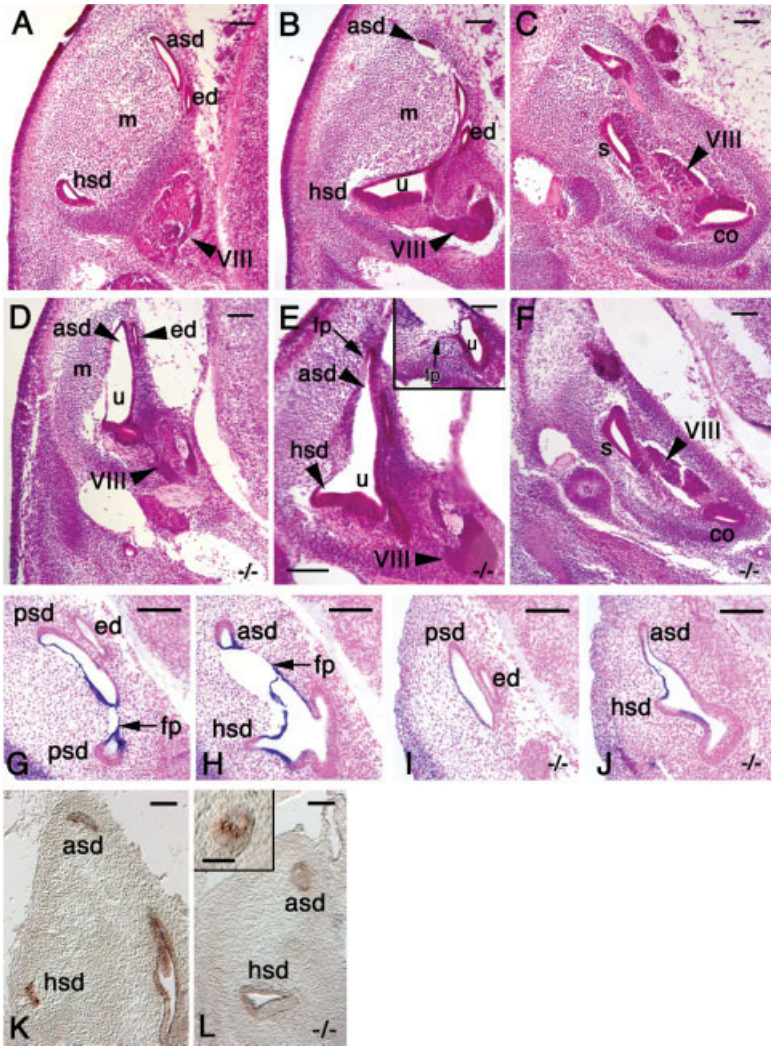

Fig. 2.

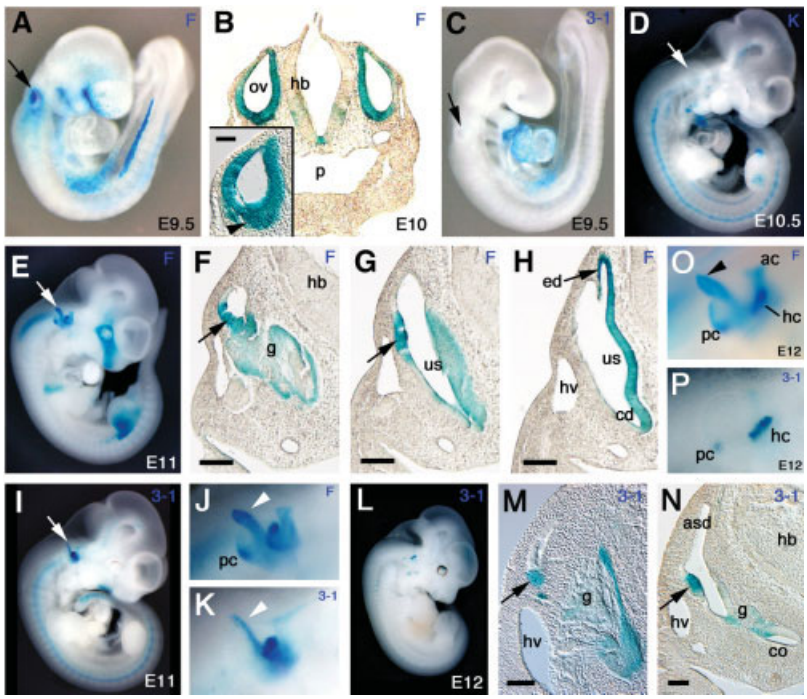

Fig. 4.

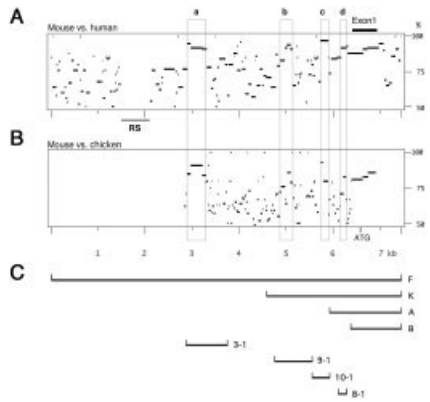

Fig. 3. **A,B:** Homology analysis of 5′ fragment of *Fgf10* between mouse and human (A) and between mouse and chicken (B). There are four conserved regions indicated by the squares in the fragment. Region "a" is an ear enhancer; regions "b", "c", and "d" were previously reported (Sasaki et al., 2002). There is a repetitive sequence (RS) element in the minus 4.5- to 5.1-kb region of the mouse *Fgf10* gene that is absent in the human genome. **C:** Schematic illustration of the constructs for generating transgenic mice. The 5′ fragment (F) was digested by restriction enzymes into three smaller fragments (*Kpn*I for K; *Apa*I for A, *Bam*HI for B, 0.2 kb). The restriction enzyme fragments containing regions "a" to "d" were designated as 3-1, 9-1, 10-1, and 8-1, respectively.

(Fekete et al., 1997). Therefore, FGF10 may be involved in cell migration and death during the removal of semicircular fused cells at the cellular level. Furthermore, recent studies have shown that a canal genesis zone is present adjacent to each prospective crista (Chang et al., 2004) and that FGFs, including FGF10 in the crista promote canal development (Chang et al., 2004; Pirvola et al., 2004). Because FGF10 is an extracellular protein with a high affinity to heparin, it is conceivable to think that FGF10 secreted from the developing crista has effects on the neighboring prospective canal epithelium by means of such proteins with heparin-binding domains as netrin 1.

Sequence Analyses and Identification of the Transcriptional Regulatory Region of the *Fgf10* Gene

The dynamic expression pattern of *Fgf10* during intricate inner ear morphogenesis (Alvarez et al., 2003; Pauley et al., 2003; Wright and Mansour, 2003) prompted us to study the regu-

latory element that drives the expression in the inner ear anlage. To elucidate the regulatory network involved in organ-specific *Fgf10* expression, we compared the 5′ sequences from the human, mouse, and chicken genomes. Although human and mouse sequences are relatively well-conserved up to 6.6 kb from the initiation codon (Fig. 3A), comparison with the chicken sequence shows a highly conserved sequence (more than 75%) up to 3.7 kb (2.9- to 6.6-kb region in Fig. 3B). There are four regions where mouse sequences are highly homologous to the corresponding chicken ones, indicating the presence of conserved enhancers. The conserved region up to 2.1 kb from the initiation codon, containing regions "b", "c", and "d" is involved in limb bud-specific expression of the *Fgf10* gene, as reported previously (Sasaki et al., 2002). A region further upstream (2.9–3.3 kb; designated as region "a" in Fig. 3A,B) appears to have an inner ear-specific enhancer element leading to *Fgf10* transcription in the otic primordia, as described below.

Identification of the Mouse *Cis*-Control Elements of *Fgf10* for the Transgene Expression in the Developing Ear

To identify the minimal *cis*-control elements regulating *Fgf10* expression in the developing embryo, we obtained DNA fragments containing conserved sequences designated as 3-1, 9-1, 10-1, and 8-1 (Fig. 3C). We generated transgenic mice that had a *lacZ* reporter gene under the control of 6.6- (designated as construct F), 2.1- (K), 0.7- (A), or 0.3- (B) kb 5′ fragments of *Fgf10*. We could generate two lines of transgenic mice with construct F: lines 20 and 53. In both lines, transgene expression was similarly detected in the otic vesicle at E9.5 (Fig. 4A; line 20; not shown for line 53 at E9.5). A strong FGF10 signal was found in the otic epithelium, except for its dorsal portion, and in the emerging ganglion cells (Fig. 4B). These expression domains of *lacZ* correspond well with the localization of *Fgf10* mRNA previously reported (Pirvola et al., 2000). At E11, *lacZ* expression was found in the sensory epithelia of the semicircular, vestibular, and cochlear regions, as well as in the vestibulocochlear ganglion (Fig. 4E–H). The two transgenic lines exhibit a distinct *lacZ* expression in the endolymphatic duct, where *Fgf10* mRNA was not usually detected (Fig. 4E,H,J; Pirvola et al., 2000). On the other hand, in the transgenic embryo with construct K, the transgene was not expressed in the developing ear (n = 8; Fig. 4D;Sasaki et al., 2002). Thus, the enhancers for expression in the ear anlage seemed to be localized between −6.6 and −2.1 kb of the 5′ fragment of *Fgf10*. Therefore, we generated transgenic mice with construct 3-1, which contains the conserved "a" region (Fig. 3). In relatively early embryos with construct 3-1, to date, we could not detect *lacZ* expression in the otic anlage as revealed by whole-mount X-gal staining (Fig. 4C, n = 2 for ~E8.5, n = 2 for ~E9.5). By E11, *lacZ* expression was detected in the developing inner ear (Fig. 4I). However, the expression domains driven by the short construct were more restricted to a portion of the inner ear anlage compared with those of construct F (Fig. 4J,K): construct 3-1 has driven the expression in one side of the endolymphatic duct and developing horizontal crista, as revealed by whole-mount X-gal staining, whereas in the embryo with construct F *lacZ* expression was found in the whole domain of the endolymphatic duct and all three crista. At E12, the *lacZ* expression by construct 3-1 was observed in more restricted manner in the horizontal and posterior cristae, compared with construct F (Fig. 4L,O,P). Serial sections of a 3-1 transgenic embryo showed *lacZ* expression in the developing crista and macula, ganglion VIII neurons, and emerging organ of Corti of the cochlea (Fig. 4M,N). We found that construct 3-1 drives a distinct expression in the developing horizontal crista, because all of nine embryos examined at E12 exhibited intense *lacZ* staining in the horizontal crista as revealed by whole-mounts. These results indicate that the enhancers for expression in the sensory compartment of developing inner ears, at least in the horizontal crista, are contained in the conserved "a" region of the sequence 3-1 (Fig. 3C). Because construct F can drive the *lacZ* expression in broader domains of the inner ear primordium than construct 3-1 while construct K cannot drive the expression in the developing ear, additional enhancers for *Fgf10* expression in the inner ear anlage may be present other than the K and 3-1 sequences.

Transcriptional Regulation of the *Fgf10* Gene

Figure 5A shows the alignment of mouse, human, and chicken nucleotide sequences for fragment 3-1. A highly conserved sequence among these three species has been detected in the first half of the sequence, approximately 400 base pair long. In this 0.4-kb fragment, there are many potential enhancer elements that are presumed to be activated by homeodomain-containing proteins, POU-domain factors, zinc-finger transcription factors, TCF/LEF-1, and a SMAD-interacting protein (Table 1; Fig. 5B). Numerous mouse mutations have been identified that show defects in morphology of the inner ear, its sensory organs, or the vestibulocochlear ganglion neurons (for a review, see Fekete, 1999). For example, the semicircular canals fail to develop in *Nkx5.1* null mutants or in mice with a double knockout of *Prx1* and *Prx2* (Wang et al., 1998; Hadrys et al., 1998; ten Berge et al., 1998). The *Hoxa1* knockouts exhibit varying degrees of severity in inner ear dysmorphogenesis (Lufkin et al., 1991; Chisaka et al., 1992; Mark et al., 1993). This and other (Pauley et al., 2003) studies have shown that FGF10 is required for semicircular canal formation. Although we suggests a possibility that *Fgf10* might be transcriptionally regulated by some Prx, Hox, and Nkx proteins, further work is needed to elucidate the relationship between *Fgf10* and these transcription factors, such as detailed comparison of their expression domains and mutagenesis of the putative binding sites.

Mutations that affect the cell types and tissue of the inner ear have also been identified. The inner ear houses the sensory organs for both hearing and balance, which use the same type of cell for sensory transduction: the hair cell. This study on the *Fgf10* enhancer analysis has verified *Fgf10* ex-

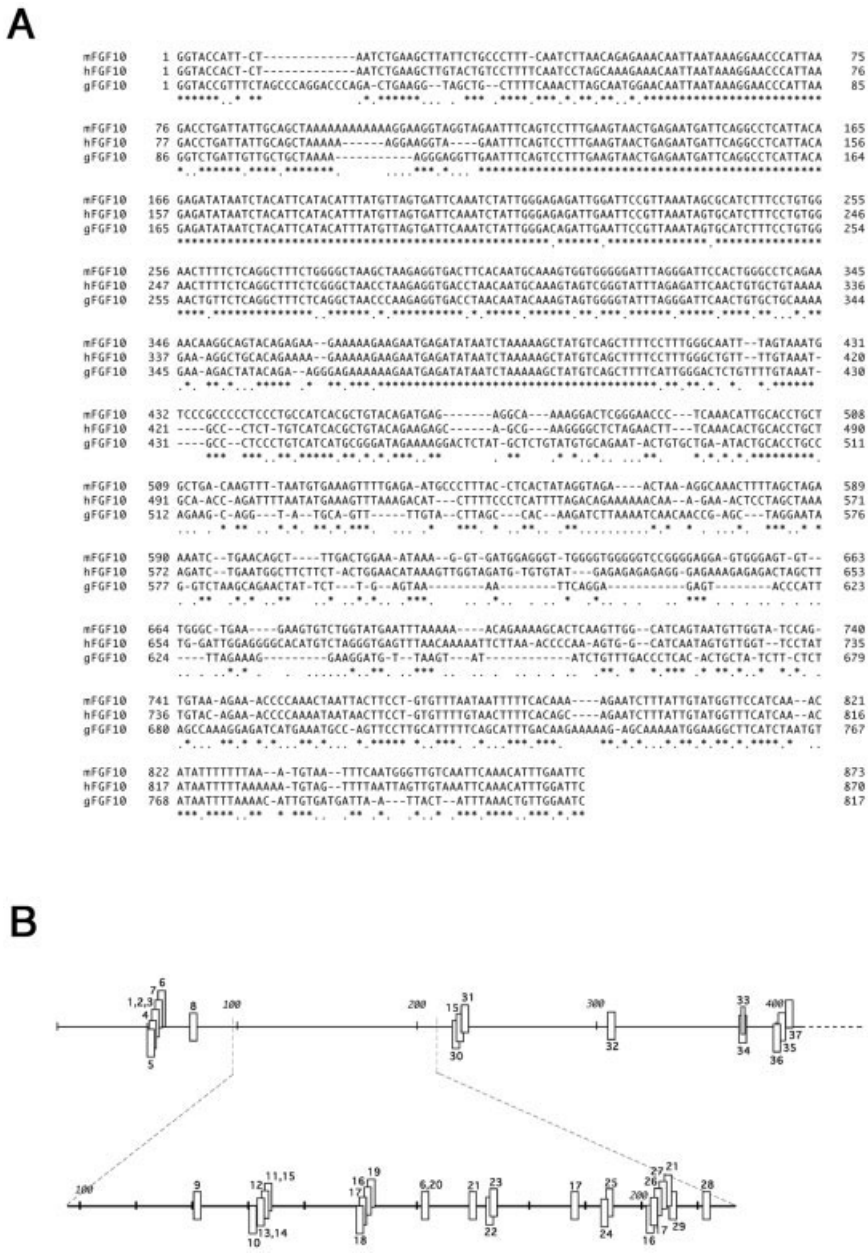

Fig. 5. **A:** Comparison of nucleotide sequences corresponding to fragment 3-1 among mouse, human, and chicken. The asterisks indicate the identical nucleotide among the three; the dot indicates where two of the three species have the same nucleotide. The 5′-half of the sequences is highly conserved among mouse, human, and chicken. **B:** Positions of DNA binding motifs conserved among mouse, human, and chicken in the 0.4-kb element of the mouse *Fgf10*. Corresponding to the 5′-half of the fragment 3-1, analyzed with MatInd and MatInspector (Quandt et al., 1995). For details, see Table 1.

pression in the sensory portion of developing otic epithelium (Pauley et al., 2003). Pauley et al. (2003) further described that the *Fgf10* null inner ear exhibited some defects in cilia formation of hair cells. Thus, it is crucial to identify upstream regulators for *Fgf10* in establishment of the otic sensory system. A mutation of *Brn3c* results in a failure of hair cells to appear in the inner ear, with subsequent loss of cochlear and vestibular ganglia (Erkman et al., 1996). Brn3a and Brn3b are also expressed in subsets of spiral and vestibular ganglion neurons (Xiang et al., 1998). On the other hand, a zinc-finger transcription factor, GATA3 is expressed in the sensory domain of the developing inner ear and involved in specification of auditory neurons (Karis et al., 2001; Lawoko-Kerali et al., 2004). Taken together with the findings of this study, it is most likely that Brn3 and GATA3 may directly regulate the expression of *Fgf10* in establishment of the otic sensory system.

Analysis of the *Fgf10* ear enhancer sequence suggests the involvement of Wnt- and BMP-signaling pathways in the regulation of *Fgf10* expression. *Bmp2* is expressed in the prospective semicircular canals (Chang et al., 2002), whereas it has been proposed that Wnt signaling gives rise to planar polarity of the outer hair cells in mammalian cochlea (Dabdoub et al., 2003). Interestingly, it was reported that the synergistic interactions of a member of FGF, FGF19, and Wnt8c initiate inner ear development (Ladher et al., 2000). Thus, it will be intriguing to clarify the specific interactions between FGF10 and these signals during inner ear development.

EXPERIMENTAL PROCEDURES

Mice

Fgf10 knockout mice were generated on a C57BL/6 X CBA background and genotyped as described (Sekine et al., 1999).

RNA In Situ Hybridization

Mouse embryos were fixed in 4% paraformaldehyde and dehydrated before embedding in paraffin or cryoprotected with 30% sucrose before embedding in O.C.T. compound. In situ hybridization was performed on 5-μm-thick paraffin sections or 18-μm-thick cryosections as described (Schaeren-Wiemers and Gerfin-Moser, 1993). A DNA fragment coding for the amino acids 25–185 of the Nkx5.1 (Hmx3) protein (Bober et al., 1994) was generated by reverse transcriptase-polymerase chain reaction (RT-PCR) from total RNA isolated from an E12.5 mouse head, cloned into pGEM-T-Easy vector (Promega), and used for preparing the probe. The template for the mouse *netrin 1* probe (nucleotides

TABLE 1. Conserved Elements of the *Fgf10* Promoter[a]

No.	Name of family	Further information	Opt.	Position from-to	Str.	Core sim.	Matrix sim.	Sequence
1	S8	Binding site for S8 type homeodomains	0.97	51–59	(+)	1	0.995	aacaATTAa
2	MSX	Homeodomain proteins MSX-1 and MSX-2	0.97	49–61	(−)	1	0.978	tatTAATtgtttc
3	BRIGHT	Bright, B cell regulator of IgH transcription	0.92	50–62	(+)	1	0.947	aaacaATTAataa
4	SOX5	Sox-5	0.87	48–64	(+)	1	0.981	agaaaCAATtaataaag
5	BRN3	POU transcription factor Brn-3	0.78	49–65	(+)	0.75	0.815	gaaACAAttaataaagg
6	HOXA5	Hox a-5, vertebrate homeobox protein	0.83	50–66	(−)	1	0.887	tcctttATTAattgttt
7	LHX3	Homeodomain binding site in LIM/homeodomain factor LHX3	0.81	53–63	(+)	1	0.851	caaTTAAtaaa
8	NKX25	Homeodomain factor Nkx-2.5/Csx, tinman homolog low affinity sites	0.88	65–77	(−)	1	0.903	tctTAATgggttc
9	TST1	POU-factor Tst-1/Oct-6	0.87	115–129	(+)	1	0.873	gtagAATTtcagtcc
10	LEF1	TCF/LEF-1, involved in the Wnt signal transduction pathway	0.94	124–140	(−)	1	0.982	gttacttCAAAggactg
11	HLF	Hepatic leukemia factor	0.84	125–145	(−)	1	0.85	tctcaGTTActtcaaaggact
12	VBP	PAR-type chicken vitellogenin promoter-binding protein	0.86	130–140	(−)	1	0.903	gTTACttcaaa
13	E4F	GLI-Krueppel—related transcription factor, regulator of adenovirus E4 promoter	0.82	131–143	(+)	0.789	0.881	ttgAAGTaactga
14	MOK2	Ribonucleoprotein-associated zinc-finger protein MOK-2 (mouse)	0.74	130–150	(−)	0.75	0.767	atcattctcagttACTTcaaa
15	VMYB	v-Myb	0.9	135–145	(+)	0.876	0.912	agtAACTgaga
16	AP1	Activator protein 1	0.95	145–155	(+)	0.846	0.961	aatgaTTCAgg
17	PIT1	Pit1, GHF-1 pituitary-specific pou domain transcription factor	0.86	145–155	(+)	1	0.919	aatgATTCagg
18	MEIS1	Homeobox protein MEIS1 binding site	0.79	146–158	(+)	1	0.793	aTGATtcaggcct
19	PAX6	Pax-6 paired domain binding site	0.75	148–166	(+)	0.754	0.821	gattcAGGCctcattacag
6	HOX1-3	Hox-1,3, vertebrate homeobox protein	0.83	154–170	(+)	1	0.853	ggcctcATTAcagagat
20	ISL1	Pancreatic and intestinal LIM-homeodomain factor	0.82	152–172	(−)	1	0.846	atatctctgTAATgaggcctg
21	GATA3	GATA-binding factor 3	0.91	164–176	(+)	1	0.958	cagAGATataatc
22	FAST1	FAST-1 SMAD interacting protein	0.81	169–183	(−)	0.983	0.869	gaatgtaGATTatat
23	CART1	Cart-1 (cartilage homeoprotein 1)	0.84	170–186	(+)	1	0.862	taTAATctacattcata
17	PIT1	Pit1, GHF-1 pituitary-specific pou domain transcription factor	0.86	180–190	(+)	0.82	0.892	attcATACatt
24	CREBP1	cAMP-responsive element binding protein	0.8	183–203	(−)	0.788	0.811	aatcactaACATaaatgtatg

Contiinues on next page.

TABLE 1. (Continued)

No.	Name of family	Further information	Opt.	Position from-to	Str.	Core sim.	Matrix sim.	Sequence
25	HNF1	Hepatic nuclear factor 1	0.8	193–209	(+)	1	0.865	tGTTAgtgattcaaatc
16	AP1	Activator protein 1	0.95	197–207	(−)	0.884	0.95	tttgaATCAct
17	PIT1	Pit1, GHF-1 pituitary-specific pou domain transcription factor	0.86	197–207	(+)	1	0.879	agtgATTCaaa
26	CHR	Cell cycle gene homology region (CDE/CHR tandem elements regulate cell cycle dependent repression)	0.92	198–210	(−)	1	0.971	agatTTGAatcac
27	PTX1	Pituitary homeobox 1 (Ptx1)	0.79	198–214	(−)	0.789	0.825	caatagaTTTGaatcac
28	CDPCR3	Cut-like homeodomain protein	0.75	199–215	(+)	0.975	0.752	tgattcaaatctATTGg
21	GATA3	GATA-binding factor 3	0.91	201–213	(−)	1	0.937	aatAGATttgaat
29	HNF6	Liver enriched Cut - Homeodomain transcription factor HNF6 (ONECUT)	0.82	203–217	(+)	0.785	0.83	tcaaaTCTAttggga
30	STAT	Signal transducers and activators of transcription	0.87	222–240	(−)	1	0.909	gctatttaacGGAAtccaa
15	VMYB	v-Myb	0.9	226–236	(−)	1	0.979	tttAACGgaat
31	EN1	Homeobox protein engrailed (en-1)	0.77	225–241	(−)	1	0.785	cgctaTTTAacggaatc
32	BARBIE	Barbiturate-inducible element	0.88	302–316	(+)	1	0.904	atgcAAAGtggtggg
33	OCT	Octamer-binding factor 1	0.9	371–385	(−)	0.944	0.926	tATATctcattcttc
34	GATA2	GATA-binding factor 2	0.9	376–388	(+)	1	0.935	atgaGATAtaatc
35	VMAF	v-Maf	0.82	388–412	(−)	1	0.878	aggaaaagcTGACatagctttttag
36	RORA2	RAR-related orphan receptor alpha2	0.82	392–408	(+)	0.75	0.831	aaagctaTGTCagcttt
37	MYT1	MyT1 zinc-finger transcription factor involved in primary neurogenesis	0.75	398–410	(−)	0.75	0.756	gaaAAGCtgacat

[a]Conserved elements in the 5′ region of the *Fgf10* promoter between mouse, human, and chicken. Numbers in the left-most column correspond to those in Figure 5B. Opt. (optimized matrix threshold): This matrix similarity is the optimized value defined in such a way that, at most, three matches are found in 10,000 bp of random DNA sequences. Position: This is shown by the number of nucleotide in the mouse, starting from the first nucleotide of fragment 3-1. Str., Strand. Core sim. (core similarity): The "core sequence" of a matrix is defined as the highest consecutive conserved positions (usually four) of the matrix. The core similarity is calculated as described in the MatInspector paper (Quandt et al., 1995). The maximum core similarity of 1.0 is only reached when the highest conserved bases of a matrix match exactly in the sequence. Matrix sim. (matrix similarity): Matrix similarity is calculated as described in the MatInspector paper (Quandt et al., 1995). A perfect match with the matrix gets a score of 1.00 (when each sequence position corresponds to the highest conserved nucleotide at that position in the matrix), a "good" match to the matrix usually has a high conservation profile (ci- value > 60). Base pairs in capital letters denote the core sequence used by MatInspector.

1431–1679) was obtained by RT-PCR and cloned into pBluescript vector (Stratagene). The digoxigenin-labeled RNA probes were prepared according to the standard procedure. The corresponding sense probes were used in parallel with antisense probes as negative controls.

Three-Dimensional Reconstruction of the Inner Ear

Eight-micrometer-thick coronal sections of the temporal region were cut with a microtome, and every sixth section was collected onto albumin-coated glass slides. They were stained with hematoxylin and eosin. The inner ear pictures were taken using a DP70 charge coupled device camera (Olympus Co., Tokyo, Japan). After adjustment of the axis of the temporal bone, outlines of the epithelial vesicle (which develops into the membranous

labyrinth) were traced for digitizing with the use of a three-dimensional reconstruction software program (Tri software; Ratoc System Co., Ltd., Tokyo, Japan).

Isolation of the 5′-Flanking Region of *Fgf10*

Mouse *Fgf10* genomic clones were isolated from a TT2 ES cell genomic library by plaque hybridization using full-length rat *Fgf10* cDNA as a probe (Sekine et al., 1999). Chicken *Fgf10* genomic clones were isolated from a chicken genomic library as previously described (Sasaki et al., 2002). We compared sequences of the mouse 6.6-kb 5′ fragment of the *Fgf10* promoter region with the corresponding regions of human and chicken *Fgf10* as a percentage identity plot (pip), which shows both the position in one sequence and the degree of similarity for each aligning segment between the two sequences (obtained with PipMaker; Schwartz et al., 2000), as illustrated in Figure 3.

Generation of Transgenic Mice and Staining for β-Galactosidase Activity

The isolated genomic clone containing a 6.6-kb 5′ upstream fragment of *Fgf10* was designated as "F" (Fig. 3C). The "F" fragment was digested with *Kpn*I, *Apa*I, and *Bam*HI into 2.1- (K), 0.7- (A), 0.3- (B) kb fragments (Fig. 3C; Sasaki et al., 2002). According to homology analysis (Fig. 3A,B), the clones 3-1, 9-1, 10-1, and 8-1 were obtained by subcloning of the restriction fragments (Fig. 3C). The analysis of clones 9-1, 10-1, and 8-1 will be reported elsewhere. To construct transgenes, each fragment was inserted into a *lacZ* reporter vector containing a promoter of the heat shock protein 68 (hsp68) and the Shine-Dalgarno-Kozak (SDK) sequence (Sasaki and Hogan, 1996).

After excision of a transgene from the vector, the concentration of the transgenes was adjusted to 500 molecules/pl and the solution was microinjected into the male pronuclei of fertilized eggs derived from superovulated BDF1 (C57BL/6 X DBA2 F1) female mice crossed with males of the same strain. Oviduct implantation of the surviving injected embryos into pseudopregnant MCH/ICR female mice was carried out according to the standard protocol. After implantation, pregnant mice were put to sleep and the embryos from E8 to E14.5 were treated with 2% paraformaldehyde for 30 min. Reporter activity was analyzed by X-gal staining overnight at 37°C. X-gal stained embryos were post-fixed in 2% paraformaldehyde, dehydrated, placed in xylene, and embedded in paraffin. The sections with a thickness of 20 μm were prepared for analysis of signals at the cellular level (Sasaki et al., 2002). The integration of the transgene into the mouse genome was detected by PCR, using primers established at the sequence of LacZ cassette and DNA extracted from tail snips of 3-week-old offspring by the proteinase K/SDS method. With construct F, two stable transgenic lines (lines 20 and 53) were obtained and had essentially the same *lacZ* expression pattern in the developing inner ear, although the expression pattern in other sites were different between the two transgenic lines. With construct K, none of transient transgenic embryos (n = 8; Fig. 4D) showed *lacZ* expression in the developing ear. As for construct 3-1, all eight of the transient transgenic embryos and one stable line obtained so far (line 1) exhibited a similar *lacZ* expression in the developing inner ear.

ACKNOWLEDGMENTS

The authors thank Dr. R. Shigemoto and his lab members for allowing us use of their equipment. We also thank C. Komaguchi for her technical assistance. The sequence of the mouse FGF10 inner ear enhancer has been deposited with DDBJ/GenBank under the accession no. AB176670, and the chicken *Fgf10* genomic sequence, including the inner ear enhancer and exon 1, under the accession no. AB176671. The materials for chicken *Fgf10* genomic DNA and mouse inner ear enhancer should be requested from T.N. Funding was provided to S.N., T.N., and H.O. by the Ministry of Education, Culture, Sports, Science, and Technology of Japan.

REFERENCES

Alvarez Y, Alonso MT, Vendrell V, Zelarayan LC, Chamero P, Theil T, Bosl MR, Kato S, Maconochie M, Riethmacher D, Schimmang T. 2003. Requirements for FGF3 and FGF10 during inner ear formation. Development 130:6329–6338.

Baker CV, Bronner-Fraser M. 2001. Vertebrate cranial placodes I. Embryonic induction. Dev Biol 232:1–61.

Boeda B, Weil D, Petit C. 2001. A specific promoter of the sensory cells of the inner ear defined by transgenesis. Hum Mol Genet 10:1581–1589.

Bober E, Baum C, Braun T, Arnold HH. 1994. A novel NK-related mouse homeobox gene: expression in central and peripheral nervous structures during embryonic development. Dev Biol 162: 288–303.

Chang W, ten Dijke P, Wu DK. 2002. BMP pathways are involved in otic capsule formation and epithelial-mesenchymal signaling in the developing chicken inner ear. Dev Biol 251:380–394.

Chang W, Brigande JV, Fekete DM, Wu DK. 2004. The development of semicircular canals in the inner ear: role of FGFs insensorycristae.Development131:4201–4211.

Chisaka O, Musci TS, Capecchi MR. 1992. Developmental defects of the ear, cranial nerves and hindbrain resulting from targeted disruption of the mouse homeobox gene Hox-1.6. Nature 355:516–520.

Dabdoub A, Donohue MJ, Brennan A, Wolf V, Montcouquiol M, Sassoon DA, Hseih JC, Rubin JS, Salinas PC, Kelley MW. 2003. Wnt signaling mediates reorientation of outer hair cell stereociliary bundles in the mammalian cochlea. Development 130:2375–2384.

De Moerlooze L, Spencer-Dene B, Revest J, Hajihosseini M, Rosewell I, Dickson C. 2000. An important role for the IIIb isoform of fibroblast growth factor receptor 2 (FGFR2) in mesenchymal-epithelial signalling during mouse organogenesis. Development 127:483–492.

Erkman L, McEvilly RJ, Luo L, Ryan AK, Hooshmand F, O'Connell SM, Keithley EM, Rapaport DH, Ryan AF, Rosenfeld MG. 1996.Role of transcription factors Brn-3.1 and Brn-3.2 in auditory and visual system development. Nature 381: 603–606.

Fekete DM, Homburger SA, Waring MT, Riedl AE, Garcia LF. 1997. Involvement of programmed cell death in morphogenesis of the vertebrate inner ear. Development 124:2451–2461.

Fekete DM. 1999. Development of the vertebrate ear: insights from knockouts and mutants. Trends Neurosci 22:263–269.

Hadrys T, Braun T, Rinkwitz-Brandt S, Arnold HH, Bober E. 1998. Nkx5-1 controls semicircular canal formation in the mouse inner ear. Development 125:33–39.

Karis A, Pata I, van Doorninck JH, Grosveld F, de Zeeuw CI, de Caprona D, Fritzsch B. 2001. Transcription factor

GATA-3 alters pathway selection of olivocochlear neurons and affects morphogenesis of the ear. J Comp Neurol 429:615–630.

Ladher RK, Anakwe KU, Gurney AL, Schoenwolf GC, Francis-West PH. 2000. Identification of synergistic signals initiating inner ear development. Science 290: 1965–1967.

Lawoko-Kerali G, Rivolta MN, Lawlor P, Cacciabue-Rivolta DI, Langton-Hewer C, van Doorninck JH, Holley MC. 2004. GATA3 and NeuroD distinguish auditory and vestibular neurons during development of the mammalian inner ear. Mech Dev 121:287–299.

Lufkin T, Dierich A, LeMeur M, Mark M, Chambon P. 1991. Disruption of the Hox-1.6 homeobox gene results in defects in a region corresponding to its rostral domain of expression. Cell 66:1105–1119.

Mansour SL, Goddard JM, Capecchi MR. 1993. Mice homozygous for a targeted disruption of the proto-oncogene int-2 have developmental defects in the tail and inner ear. Development 117:13–28.

Mark M, Lufkin T, Vonesch JL, Ruberte E, Olivo JC, Dolle P, Gorry P, Lumsden A, Chambon P. 1993. Two rhombomeres are altered in Hoxa-1 mutant mice. Development 119:319–338.

Martin P, Swanson GJ. 1993. Descriptive and experimental analysis of the epithelial remodellings that control semicircular canal formation in the developing mouse inner ear. Dev Biol 159:549–558.

Min H, Danilenco DM, Scully SA, Bolon B, Ring BD, Tarpley JE, DeRose M, Simonet WS. 1998. FGF10 is required for both limb and lung development and exhibits striking functional similarity to Drosophila branchless. Genes Dev 12:3156–3161.

Morsli H, Choo D, Ryan A, Johnson R, Wu DK. 1998. Development of the mouse inner ear and origin of its sensory organs. J Neurosci 18:3327–3335.

Murakami A, Ishida S, Thurlow J, Revest JM, Dickson C. 2001. SOX6 binds CtBP2 to repress transcription from the Fgf-3 promoter. Nucleic Acids Res 29:3347–3355.

Noramly S, Grainger RM. 2002. Determination of the embryonic inner ear. J Neurobiol 53:100–128.

Ohuchi H, Hori Y, Yamasaki H, Sekine K, Kato S, Itoh N. 2000. FGF10 acts as a major ligand for FGF receptor 2 IIIb in mouse multi-organ development. Biochem Biophys Res Commun 277:643–649.

Ornitz DM, Xu J, Colvin JS, McEwen DG, MacArthur CA, Coulier F, Gao G, Goldfarb M. 1996. Receptor specificity of the fibroblast growth factor family. J Biol Chem 271:15292–15297.

Pauley S, Wright TJ, Pirvola U, Ornitz D, Beisel K, Fritzsch B. 2003. Expression and function of FGF10 in mammalian inner ear development. Dev Dyn 227:203–215.

Pirvola U, Spencer-Dene B, Xing-Qun L, Kettunen P, Thesleff I, Fritzsch B, Dickson C, Ylikoski J. 2000. FGF/FGFR-2(IIIb) signaling is essential for inner ear morphogenesis. J Neurosci 20:6125–6134.

Pirvola U, Zhang X, Mantela J, Ornitz DM, Ylikoski J. 2004. Fgf9 signaling regulates inner ear morphogenesis through epithelial-mesenchymal interactions. Dev Biol 273:350–360.

Quandt K, Frech K, Karas H, Wingender E, Werner T. 1995. MatInd and MatInspector: new fast and versatile tools for detection of consensus matches in nucleotide sequence data. Nucleic Acids Res 23:4878–4884.

Represa J, Leon Y, Miner C, Giraldez F. 1991. The int-2 proto-oncogene is responsible for induction of the inner ear. Nature 353:561–563.

Rinkwitz S, Bober E, Baker R. Development of the vertebrate inner ear. 2001. Ann N Y Acad Sci 942:1–14.

Salminen M, Meyer BI, Bober E, Gruss P. 2000. Netrin 1 is required for semicircular canal formation in the mouse inner ear. Development 127:13–22.

Sasaki H, Hogan BL. 1996. Enhancer analysis of the mouse HNF-3 beta gene: regulatory elements for node/notochord and floor plate are independent and consist of multiple sub-elements. Genes Cells 1:59–72.

Sasaki H, Yamaoka T, Ohuchi H, Yasue A, Nohno T, Kawano H, Kato S, Itakura M, Nagayama M, Noji S. 2002. Identification of cis-elements regulating expression of *Fgf10* during limb development. Int J Dev Biol 46:963–967.

Schaeren-Wiemers N, Gerfin-Moser A. 1993. A single protocol to detect transcripts of various types and expression levels in neural tissues and cultured cells: in situ hybridization using digoxigenin-labelled cRNA probes. Histochemistry 100:431–440.

Schwartz S, Zhang Z, Frazer KA, Smit A, Riemer C, Bouck J, Gibbs R, Hardison R, Miller W. 2000. PipMaker—a web server for aligning two genomic DNA sequences. Genome Res 10:577–586.

Sekine K, Ohuchi H, Fujiwara M, Yamasaki M, Yoshizawa T, Sato T, Yagishita N, Matsui D, Koga Y, Itoh N, Kato S. 1999. *Fgf10* is essential for limb and lung formation. Nat Genet 2:1138–1141.

Takuma N, Sheng HZ, Furuta Y, Ward JM, Sharma K, Hogan BL, Pfaff SL, Westphal H, Kimura S, Mahon KA. 1998. Formation of Rathke's pouch requires dual induction from the diencephalon. Development 125:4835–4840.

ten Berge D, Brouwer A, Korving J, Martin JF, Meijlink F. 1998. Prx1 and Prx2 in skeletogenesis: roles in the craniofacial region, inner ear and limbs. Development 125:3831–3842.

Uchikawa M, Ishida Y, Takemoto T, Kamachi Y, Kondoh H. 2003. Functional analysis of chicken Sox2 enhancers highlights an array of diverse regulatory elements that are conserved in mammals. Dev Cell 4:509–519.

Vendrell V, Carnicero E, Giraldez F, Alonso MT, Schimmang T. 2000. Induction of inner ear fate by FGF3. Development 127:2011–2019.

Wang W, Van De Water T, Lufkin T. 1998. Inner ear and maternal reproductive defects in mice lacking the Hmx3 homeobox gene. Development 125:621–634.

Wright TJ, Mansour SL. 2003. Fgf3 and Fgf10 are required for mouse otic placode induction. Development 130:3379–3390.

Wright TJ, Ladher R, McWhirter J, Murre C, Schoenwolf GC, Mansour SL. 2004. Mouse FGF15 is the ortholog of human and chick FGF19, but is not uniquely required for otic induction. Dev Biol 269: 264–275.

Xiang M, Gao WQ, Hasson T, Shin JJ. 1998. Requirement for Brn-3c in maturation and survival, but not in fate determination of inner ear hair cells. Development 125:3935–3946.